International Journal of Applied Information Systems (IJAIS) – ISSN : 2249-0868
Foundation of Computer Science FCS, New York, USA
Volume 12– No. 44, May 2024 – www.ijais.org

Beyond Binary Diagnostics of Pneumonia Detection with Deep Learning

Olukemi Victoria Olatunde
Department of Software Engineering
Federal University of Technology, Akure

Olumide Sunday Adewale
Department of Computer Science
Federal University of Technology, Akure

Parimala Thulasiraman
Department of Computer Science
University of Manitoba, Winnipeg
Manitoba, Canada

Oladunni Abosede Daramola
Department of Information Technology
Federal University of Technology, Akure

ABSTRACT
Pneumonia has been a major public health issue throughout human history and is among the common symptoms of the virus that causes COVID-19, which has turned into a worldwide pandemic. The disease is especially prevalent in developing countries, with Nigeria being one of the five countries accounting for more than half of the world's annual incident cases of pneumonia. In 2015, Nigeria recorded 2,300 deaths among children under five due to pneumonia, and it is projected that two million could die in the next decade if no action is taken. The disease wreaks havoc in areas where the doctor-to-patient ratio is low, causing deaths primarily in children under five years old and elderly people over 65 years old, particularly those with weakened immune systems. Pneumonia is the leading infectious cause of death in children worldwide, with higher incidence rates in developing countries due to poor sanitary conditions and poverty. Deep learning techniques, particularly Convolutional Neural Networks (CNNs) using X-ray images, have significantly contributed to pneumonia diagnosis. However, previous studies have only focused on distinguishing between healthy and pneumonia patients without considering the severity level. In developing countries, physicians using these machine learning tools are unable to determine the severity of pneumonia, resulting in patients with moderate pneumonia not receiving adequate care. Although this approach is cost-effective for the healthcare system, it is dangerous for the patients. In this study, a deep learning model is proposed to complement the work of physicians by determining the severity level of pneumonia after confirming the infection through X-ray.

Keywords
Pneumonia, Severity, HOG, CNN, X-ray images, Pearson Correlation

1. INTRODUCTION
Accessing medical facilities is of vital importance for individuals facing health challenges to receive proper medical diagnosis and timely treatment. However, this can be a significant challenge in developing countries where poverty and a shortage of medical personnel are prevalent, resulting in increased mortality rates due to the lack of funds to access available medical facilities [1]. Recently, Artificial Intelligence (AI) has been employed in solving medical problems; expert systems, machine learning, and deep learning are a few examples of the techniques used. Deep learning, a subset of machine learning, consists of algorithms inspired by the functioning of the human brain. It teaches computers to perform tasks that come naturally to humans by allowing input data to be classified directly based on raw input rather than constructing features manually. Deep learning models can achieve state-of-the-art accuracy, sometimes exceeding human-level performance [2].

Pneumonia is an infection of one or both lungs caused by bacteria, viruses, or fungi, in which the air sacs are filled with pus. Before the outbreak of the COVID-19 pandemic, it was the single largest infectious cause of death in children under five years of age, claiming more lives than any other infectious disease worldwide. It claimed the lives of over 700,000 children under five every year, including over 200,000 newborns, with approximately 2,000 deaths per day, resulting in the death of a child from pneumonia every 43 seconds. Pneumonia is also the fourth leading cause of death across all ages. In 2019, pneumonia killed 740,180 children under the age of five, accounting for 14% of all deaths in this age group [3-7].

Pneumonia affects children and families everywhere, but it is more prominent in developing countries. Nigeria, as a case study, is one of the five countries with more than half of the world's annual incident cases of pneumonia, recording 2,300 under-five deaths in 2015. The country had the highest number of child mortalities, with an estimated 162,000 deaths in 2018, approximately 443 deaths per day, with pneumonia accounting for 19% of these deaths. It is projected that two million children could die in the next decade if nothing is done to help curtail the disease [8-10].

Hence, there is a need for early diagnosis and, most importantly, the need to understand the extent of damage the disease has done to the patient's body in terms of severity. This is essential for providing timely and appropriate priority treatments and medications for pneumonia patients to curb the menace of this disease.

X-ray images have been a common tool employed for pneumonia diagnosis, and this requires the service of an expert radiologist to interpret the X-ray [11]. However, as there are lots of respiratory diseases sharing similar features with pneumonia, this sometimes leads to subjectivity in the interpretation. This subjectivity in interpretation highlights the need for a computer-aided diagnostic system for accurate interpretation [12].

This paper proposes a deep learning model to assist medical experts in diagnosing the severity of pneumonia. A Histogram of Oriented Gradients (HOG) feature descriptor, Pearson

correlation, and CNN were employed on Kaggle's Chest X-ray images. Figure 1 shows the lungs of a healthy air sacs versus pneumonia infested air sacs, and Figure 2a shows the X-ray images of normal patients, and 2b the X-ray images of pneumonia patients.

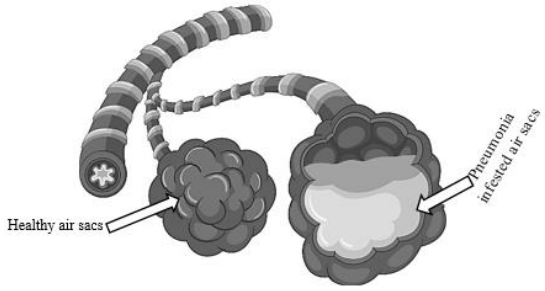

Figure 1: Healthy air sacs versus pneumonia infested air (adapted from [13])

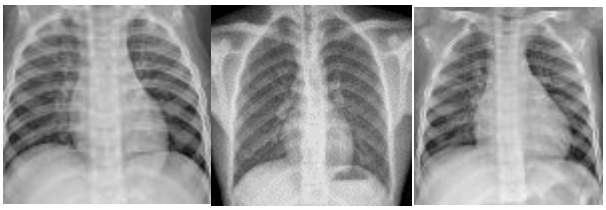

Figure 2a: Normal X-ray images

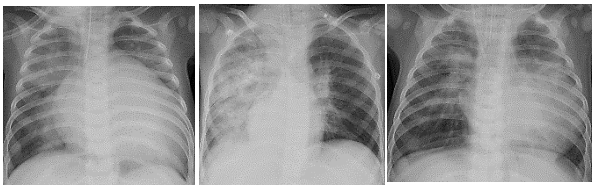

Figure 2b: Pneumonic X-ray images

Pneumonia can develop in patients already in the hospital for other sicknesses. It can be spread through coughing, sneezing, or by touching infected shared objects. Signs and symptoms of pneumonia include fever, chills, cough, shortness of breath, and fatigue. Pneumonia symptoms vary from mild to severe, depending on factors such as the type of germ causing the infection, age, and overall health of the patients. Mild signs and symptoms are often similar to those of a cold or flu, but they last longer. Some of the pneumonia signs and symptoms include:

• Chest pain when breathing or coughing

• Confusion or changes in mental awareness (in adults age 65 and older)

• Cough, which may produce phlegm or pus

• Fatigue

• Persistent fever of 102°F (39°C) or higher

• Sweating and shaking chills

• Lower than normal body temperature (in adults older than age 65 and people with weak immune systems)

• Nausea, vomiting, or diarrhea

• Difficult breathing

Pneumonia may also present itself in the elderly with confusion and lack of fever. Patients with severe symptoms experience loss of appetite, bodily discomfort, and sometimes coughing up blood [14].

Cough, fever, dyspnea, and crackles on examination, are suggestive pneumonia symptoms but they are not evident as they share symptoms with other lower respiratory system diseases. Automating the severity diagnosis of infected pneumonia patients will ensure accurate diagnosis and assist in prioritizing pneumonia treatment to improve health care in resource-scarce areas like Africa, reducing the mortality rate of the disease.

The main contribution of this work is to propose a pneumonia severity diagnosis model that will be beneficial in developing areas, specifically, Nigeria, where the doctor-to patient ratio stands at 1:9083 instead of the recommended 1:600 as stated in [15] and to serve as a specialists' supporting tool for diagnosis and decisions making.

In this study, publicly available pneumonia dataset used by Kermany in [16] was used.

The rest of this paper is organized as follows. Section II discusses related work on pneumonia diagnosis, Deep Learning, and Histogram of Oriented Gradient. Our proposed model technique is discussed in Section III. The experimental setup is outlined in Section IV and Section V discusses the results. Section VI concludes the paper with future work.

2. RELATED WORKS

In recent years, artificial intelligence methods have been employed in the diagnosis of various diseases. A fuzzy expert system for pneumonia diagnosis was developed in [17]. A CNN deep learning model for the detection and classification of ear infections was proposed in [18]; A deep learning based pneumonia severity diagnosis model that can assist medical practitioners in prioritizing pneumonia patients' treatment was proposed by Olatunde in [19]. An intelligent deep transfer-learning-based malaria parasite detection and classification (IDTL-MPDC) model that can determine malaria presence from blood smear images using median filtering was developed in [20]. An Intelligent system for detecting COVID-19 was developed by combining features extracted from histogram-oriented gradient (HOG) and Convolutional Neural Networks (CNN) in [21].

The development and application deep learning especially the use of CNN in medical image analysis have made deep learning-based diagnosis a feasible method. Barbosa and Canuto in [22] proposed a custom machine learning model. The model used HOG in extracting features from chest X-ray images to classify and detect the presence of pneumonia. If pneumonia is detected, the model further classified the detected pneumonia as either caused by viral or bacterial infection. A supervised computer-aided diagnostic (CAD) system for the binary classification of chest X-ray images into pneumonia or normal was presented in [23]. The CAD system processed hundreds of X-rays images by using the HOG to extract features from the X-ray images which were further classified using Support Vector Machine (SVM), decision tree and random forest techniques.

As a result of high mortality and morbidity rate of pneumonia especially in children and the complication accompanying

those with severe condition, a CNN and VGG16 models that can assist radiologists in improving the diagnostic accuracy of pulmonary diseases using chest X-ray was proposed in [24]. Siddiqi et al., 2019 presented a deep learning based model that classify chest X-rays into 'normal' and 'pneumonia' was presented by Siddiqi in [25]. [26] employed four different CNN-based deep transfer learning algorithms (i.e. VGG19, Xception, ResNet50, and DenseNet121) in the automatic classification of chest X-ray radiography into healthy and pneumonia. Similar ideas from [26] was adopted in [27] by combining CNN and deep learning algorithms such as VGG16, VGG19, and Xception transfer learning to detect COVID-19-induced pneumonia from chest X-rays.

3. PROPOSED METHODOLOGY FOR SEVERITY DETECTION

Upon reviewing related literature, it became evident that existing diagnostic systems for pneumonia are binary, merely indicating whether a patient has the condition or not. However, considering the constraints of healthcare access and diagnostic resources, understanding the severity of the disease is imperative as this knowledge facilitates tailored treatment plans, the prescription of suitable medications to prevent complications, and ultimately enhances patient outcomes while minimizing transmission risks. It will also aid public health agencies in identifying trends, allocating resources efficiently, and devising targeted interventions and prevention strategies.

The architecture of the proposed Deep Learning Model for Pneumonia Severity Diagnosis is presented in Figure 3 is characterized by a chest X-ray image dataset, Image preprocessing stage, Feature extraction module, Dataset Splitting, Target categorization module, the training module and the Evaluation module.

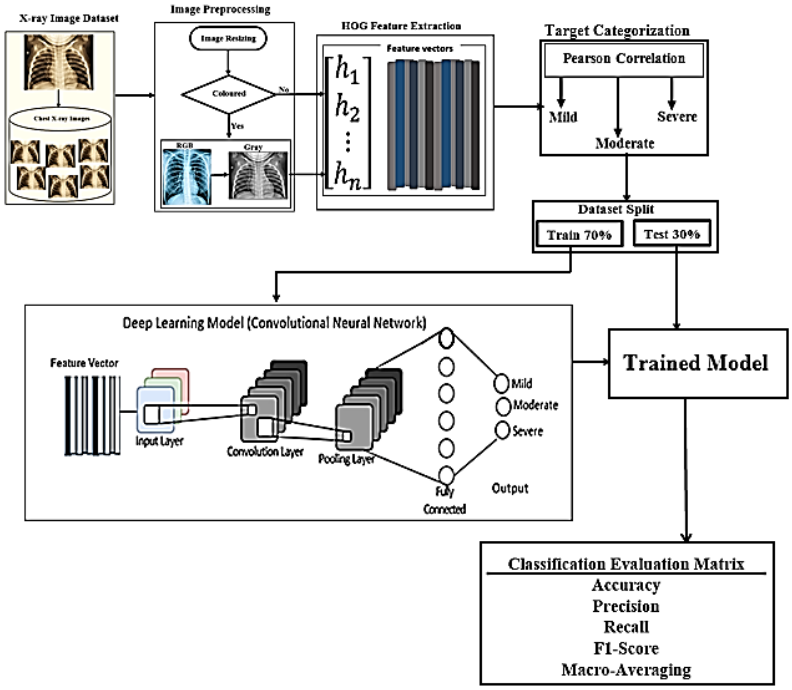

Figure 3: Architecture of the Pneumonia Detection with Deep Learning

3.1 Image Dataset

The "Pneumonia Detection with Deep Learning" utilized a publicly available dataset from Kaggle, comprising 5,856 chest X-rays labeled as either Pneumonia or Normal. These X-rays were drawn from pediatric patients aged one to five years old at the Guangzhou Women and Children's Medical Center. The Pneumonia dataset includes both Bacterial and Viral Pneumonia X-ray images. Normal X-rays depicts clear lungs as illustrated in Figure 4, Pneumonia-infested X-ray images typically show focal lobar consolidation, as seen in Figure 5.

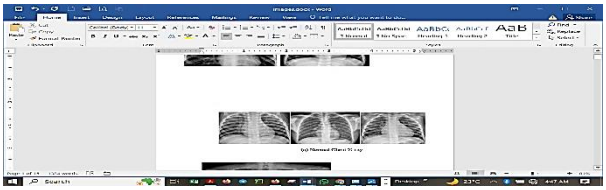

Figure 4: Random samples of Normal X-ray images

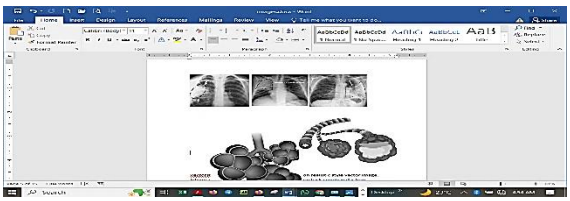

Figure 5: Random samples of Pneumonia-infested X-ray images

3.2 Image Preprocessing

This is achieved by resizing the input X-ray image to 128 x 64 pixels (128 pixels' height and 64 pixels' width). The size was chosen as the image will be divided into 8x8 and 16x16 patches to extract the features, and also to conform with the values used in the original paper.

3.3 Feature Extraction

HOG Features were extracted from both the Normal and Pneumonia X–ray grayscale images using the following steps:

a. **Gradient Computation**: For every single pixel in the 128 x 64 pixels cell, both the magnitude and orientation of the gradient in both the horizontal $t_x(x,y)$ and the vertical $t_y(x,y)$ directions are calculated by employing a 1-D discrete derivative mask centered around a pixel of every image patches using convolution operation with $t_x(x,y) = [1 \quad 0 \quad -1]$, and $t_y(x,y) = [1 \quad 0 \quad -1]^T$ filtering kernel as defined in Equation (1) and Equation (2) respectively.

$$t_x(x,y) = |l(x-1,y) - l(x+1,y)| \qquad (1)$$

$$t_y(x,y) = |l(x,y-1) - l(x,y+1)| \qquad (1)$$

Where $x = 1 \ldots 64;\ \ y = 1 \ldots 28$

The two computed gradients are used in computing the gradient magnitudes and angles

b. **Computation of gradient magnitude and angle**: For each pixel $t(x,y)$ the intensity value in the gradient magnitude and the gradient angle and orientation are computed using Equation (3) and Equation (4) respectively. The gradient is then transformed to polar coordinates with the angle between 0^o and 180^o

$$\mu = \sqrt{t_x(x,y)^2 + t_x(x,y)^2} \qquad (3)$$

$$\alpha = tan^{-1}\left(\frac{t_x(x,y)}{t_y(x,y)}\right) \qquad (4)$$

Where tan^{-1} is the inverse tangent; which yields values between $-\pi$ and π, and μ and α denote the magnitude and the direction (angle) of the gradient of each pixel respectively

c. **Building the Histogram**: After obtaining the gradient of each pixel, the gradient matrices (magnitude and angle) are divided into 8x8 cells to form a block. For each block, an evenly spaced 0^o to 180^o 9-point histogram with each bin having an angle range of 20 degrees representing the distribution of gradient orientations within the cell was calculated. Each pixel calculates a weighted vote for an edge orientation histogram channel based on the orientation of the gradient element centered on it, and the votes are accumulated into orientation bins over local spatial regions called cells.

d. **Block normalization**: The histograms are normalized to reduce the system's sensitivity to overall lighting. This is accomplished by dividing the blocks spanning 2 x 2 cells. The l_2 normalization is done on (16 x 16) blocks with 0 overlaps containing four (8 x 8 pixels) histograms of gradients as shown in Figure 6. The histograms are concatenated to generate an array of size (1 x 36).

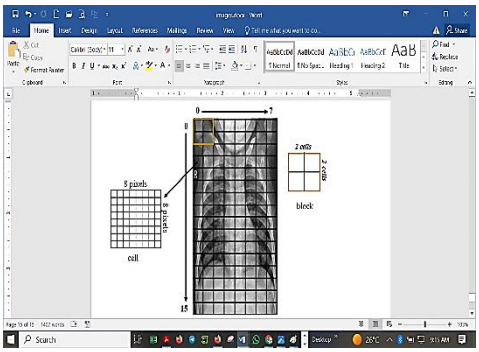

Figure 6: Non-overlapping partitioning of an X-ray image

For a vector $H = [h_1, h_2, h_3, \cdots, h_n]$, where H is the feature of the block, and h_i is the histogram of the cell (i). The l_2 norm of the vector is calculated as in Equation (5) and Equation (6) respectively

$$H_{l_2} = |H| = \sqrt{h_1^2 + h_2^2 + h_3^2 + \cdots + h_n^2 + \epsilon} \qquad (5)$$

Where ϵ is a small positive constant preventing division by zero in gradient-free blocks.

$$H_{norm} = \frac{H}{|H|} \qquad (6)$$

e. **HOG Feature**: All the normalized block features H_{norm} are concatenated to produce one HOG that represents the whole window features for a chest X-ray image. The process is repeated for all the X-ray images.

3.4 Dataset Splitting

The dataset was acquired from Kaggle website https://www.kaggle.com/datasets/paultimothymooney/chest-xray-pneumonia, and was divided into a 70-30 proportion for the training and testing sets, respectively. The training dataset was utilized to fit the model, while the algorithm made predictions using the test set. These predictions were then evaluated against the labels obtained from target categorization to measure the efficiency of the method.

The dataset comprised a total of 5216 X-ray images, with 3875 images depicting confirmed cases of pneumonia and 1341 images showing healthy individuals. The normal images served as a baseline for determining the severity of the pneumonia images. Subsequently, the pneumonia images, after being reclassified into severity classes, were split into training (2712) and testing (1163) sets for training using Convolutional Neural Network (CNN) as shown in Table 1.

Table 1: Number of images present in each class

Normal	1341		
Pneumonia	3875	**Train** (70%)	**Test** (30%)
		2713	1163
Total	5216		

3.5 Target Categorization

To determine the significance of the relationship between the Normal and Pneumonia X-ray images, the feature vectors from both Normal and Pneumonia X-ray images are passed through Pearson correlation, and the magnitude of the strength between the randomly picked Normal X-ray image feature vector and all the Pneumonia X-ray images feature vectors is computed using

the Pearson correlation as in Equation (7) which is used to describe the strength and direction of an association between variables.

$$r_{np} = \frac{\sum(n_i - \bar{n})\,(p_i - \bar{p})}{\sqrt{\sum(n_i - \bar{n})^2 \sum(p_i - \bar{p})^2}} \quad (7)$$

Where r_{np} is the correlation between normal and pneumonia X-ray images feature vectors; n_i is the value of a randomly picked extracted Normal X-ray image HOG features vector; $\bar{n}$ is the mean value of the Normal X-ray images features vectors; p_i values of the extracted pneumonia X-ray image HOG features vector; $\bar{p}$ is the mean value of Pneumonia X-ray images features vectors.

From the literature reviewed, it is evident that no system has been designed for pneumonia severity classification; thus, there is no baseline to use as a standard. Based on the correlation strengths, different thresholds were selected for the severity levels, and the models were subsequently trained and evaluated according to these thresholds. The pneumonia images are classified into severity groups using Equation (8) through Equation (10).

$$f(s) = \begin{cases} Severe & if\ s < 0.3 \\ Moderate & if\ 0.3 \le s < 0.5 \\ Mild & if\ s \ge 0.5 \end{cases} \quad (8)$$

$$f(s) = \begin{cases} Severe & if\ s < 0.4 \\ Moderate & if\ 0.4 \le s < 0.6 \\ Mild & if\ s \ge 0.6 \end{cases} \quad (9)$$

$$f(s) = \begin{cases} Severe & if\ s < 0.2 \\ Moderate & if\ 0.2 \le s < 0.5 \\ Mild & if\ s \ge 0.5 \end{cases} \quad (10)$$

3.6 Model Training

The training of the model is carried out in three major layers:

i. Convolution Layer
ii. Pooling Layer
iii. Flattened and Fully Connected Layer

Convolution Layer: A 3 x 3 filter is used to extract feature maps from the input matrix, during which the filter is multiplied by the pixels in the image vector and summed according to the formula in Equation (11).

$$x_j^i = f\left(\sum_i x_i^{i-1} * k_j^i + b_j^i\right) \quad (11)$$

Where x_j^i is the output layer feature map, $f(x)$ is an activation function, "*" is a convolution operation of input x of the map layer l; b_j^i is the coefficient of the layer l for the feature map j. Multiple filters are applied into input matrix to obtain a layer of feature map. Rectified Linear (ReLU) activation function as defined in Equation 12 is applied to the convolution layer as an active function which introduces non-linearity into the model, helping it learn from complex data.

$$f(x) = \begin{cases} 0, & x < 0 \\ x, & x \ge 0 \end{cases} \quad (12)$$

Pooling: Max-pooling depicted by Equation 13 used in reducing the spatial dimensions of the feature maps, while preserving the depth by selecting the highest value of the feature map, and provides the salient features was employed in this study. This works by dividing the input feature map into a set of non-overlapping regions, called pooling regions. Each pooling region is then transformed into a single output value, which represents the presence of a particular feature in that region.

$$Y_{i,j} = max_{m,n} X_{i \cdot s+m, j \cdot s+n} \quad (13)$$

Where $Y_{i,j}$ is the output feature map at position (i, j); $X_{i \cdot s+m, j \cdot s+n}$ is the input feature map value at position $(i \cdot s + m, j \cdot s + n)$, s is the stride of the pooling operation; m and n are indices that iterate over the pooling window, and max is the maximum operation applied over all the values within the pooling window.

Flattening and Fully Connected Layer: After pooling, the feature map is processed through a flattening and fully connected layer. In this step, the pooled features are reshaped into a single column to be fed into the neural network. Subsequently, this flattened feature map is passed into the fully connected layer, where the network makes predictions based on the input. In the deep learning training model, a confirmed pneumonia chest X-ray image is classified into one of the label classes based on its severity group: Mild, Moderate, or Severe, as stated in Equations (8) to (10).

3.7 Trained Model

Here, a set of Test images will be passed through the trained model for model evaluation

3.8 Classification Evaluation Matrix

Four evaluation metrics Accuracy, Precision, Recall, and F1-score with four indices, True Positive (TP), True Negative (TN), False Positive (FP), and False Negative (FN) will be used in determining the performance of the deep learning model for pneumonia severity diagnosis, and these metrics are discussed below.

Accuracy: Accuracy measures the proportion of correctly classified cases from the total number of objects in the dataset. It is computed by dividing the number of correct predictions by the total number of predictions made by the model, and computed as in Equation (14)

$$accuracy = \frac{correct\ predictions}{total\ number\ of\ predictions} \quad (14)$$

Precision: precision measures the model's ability to identify instances of a particular class correctly, and it is computed as in Equation (15) through Equation (17)

$$precision_{Mild} = \frac{TP_{Mild}}{TP_{Mild} + FP_{Mild}} \quad (15)$$

$$precision_{Mod} = \frac{TP_{Moderate}}{TP_{Moderate} + FP_{Moderate}} \quad (16)$$

$$precision_{Sev} = \frac{TP_{Severe}}{TP_{Severe} + FP_{Severe}} \quad (17)$$

Recall: This measures the model's ability to identify all instances of a particular severity class, and it is computed as in Equation (18) through (20)

$$recall_{Mild} = \frac{TP_{Mild}}{FP_{Mild} + FN_{Mild}} \quad (18)$$

$$recall_{Mod} = \frac{TP_{Moderate}}{FP_{Moderate} + FN_{MModerate}} \quad (19)$$

$$recall_{Sev} = \frac{TP_{Severe}}{FP_{Severe} + FN_{Severe}} \quad (20)$$

F1 score: This is the harmonic mean of the precision and recall of a specific severity class, and is computed as shown in Equation (21) through Equation (23)

$$F1_{Mild} = 2 \times \frac{precision_{Mild} \times recall_{Mild}}{precision_{Mild} + recall_{Mild}} \quad (21)$$

$$F1_{Mod} = 2 \times \frac{precision_{Mod} \times recall_{Mod}}{precision_{Mod} + recall_{Mod}} \quad (22)$$

$$F1_{Sev} = 2 \times \frac{precision_{Sev} \times recall_{Sev}}{precision_{Sev} + recall_{Sev}} \quad (23)$$

Macro Averaging: This shows average performance across classes, treating each class as equally important. It is computed by Averaging the precision and recall across all classes to get the final macro-averaged precision and recall scores. Equation (24) and Equation (25) shows Macro Averaged precision and recall calculation respectively.

$$precision_{Macro-avg} = \frac{Precision_{Mild} + Precision_{Mod} + Precision_{Sev}}{3} \quad 24$$

$$Recall_{Macro-avg} = \frac{Recall_{Mild} + Recall_{Mod} + Recall_{Sev}}{3} \quad 25$$

Macro-Average F1 Score: This computes a single model performance indicator by averaging the precision and recall scores of individual classes, and using the computed global precision and recall scores to compute global F1 score. Macro-Average F1 score is computed using Equation (26).

$$F1 = 2 \times \frac{Gprecision \times Grecall}{Gprecision + Grecall} \quad 26$$

Where

$Gprecision = \frac{1}{n}\sum_{i=1}^{n} precision;\ \ Grecall = \frac{1}{n}\sum_{i=1}^{n} recall,$ and $n = No\ of\ severity\ classes$

TP (True Positive) is when a classifier correctly predicts the existence of a severity label.

TN (True Negative) is when a classifier correctly predicts the in-existence of a severity label

FP (False Positive) is when a classifier predicts a label that does not exist in the input image.

FN (False Negative) is when a classifier misses a label that exists in the input image.

4. CONCLUSION

Existing work focuses on classifying chest X-ray images as either healthy or pneumonia-affected. This study proposes to address a more complex problem by classifying X-ray images into various severity levels, which will complement and improve priority decisions made by medical experts, with the ultimate aim of reducing the pneumonia mortality rate. In this paper, the Histogram of Oriented Gradients (HOG) feature descriptor, Pearson Correlation, and a Convolutional Neural Network (CNN) built from scratch are used to diagnose pneumonia severity levels in X-ray images. Although the model has not been fully implemented, it can aid radiologists in decision-making. For future work, the researchers plan to complete the model implementation on larger dataset for improved efficiency.

5. REFERENCES

[1] Ortiz-Toro, C., García-Pedrero, A., Lillo-Saavedra, M., & Gonzalo-Martín, C. (2022). Automatic detection of pneumonia in chest X-ray images using textural features. Computers in biology and medicine, 145, 105466.

[2] Kumar, Y., Koul, A., Singla, R., & Ijaz, M. F. (2023). Artificial intelligence in disease diagnosis: a systematic literature review, synthesizing framework and future research agenda. Journal of ambient intelligence and humanized computing, 14(7), 8459–8486.

[3] Beletew, B., Bimerew, M., Mengesha, A., Wudu, M., & Azmeraw, M. (2020). Prevalence of pneumonia and its associated factors among under-five children in East Africa: a systematic review and meta-analysis. BMC pediatrics, 20(1), 254.

[4] CDC. (2022) Pneumonia an infection of the lung. Accessed: 2023-06-12. [Online]. Available: https://www.cdc.gov/pneumonia/index.html.

[5] GAVI. (2022) Five charts on the growing pneumonia crisis. Accessed: 2023-06-12. [Online]. Available: https://www.gavi.org/vaccineswork/every-death-counts-pneumonia-five-charts.

[6] UNICEF. (2022) Pneumonia. Accessed: 2023-06-12. [Online]. Available: https://data.unicef.org/topic/child-health/pneumonia.

[7] Ijaz, A., Akbar, S., AlGhofaily, B., Hassan, S. A., and Saba, T. (2023). Deep Learning for Pneumonia Diagnosis Using CXR Images. 2023 Sixth International Conference of Women in Data Science at Prince Sultan University (WiDS PSU), Riyadh, Saudi Arabia, 2023, pp. 53-58.

[8] UNICEF. (2019) Nigeria contributes highest number to global pneumonia child deaths. Accessed: 2023-06-12. [Online]. Available:https://www.unicef.org/nigeria/press-releases/nigeria-contributes-highest-number-global-pneumonia-child-deaths.

[9] UNICEF. (2020) Two million children in Nigeria could die in the next decade. Accessed: 2023-12-12. [Online]. Available:https://www.unicef.org/nigeria/press-releases/two-million-children-nigeria-could-die-next-decade.

[10] WHO. (2022) Pneumonia in children. Accessed: 2023-06-12. [Online]. Available: https://www.who.int/news-room/fact-sheets/detail/pneumonia.

[11] Yao, D., Xu, Z., Lin, Y., & Zhan, Y. (2023). Accurate and intelligent diagnosis of pediatric pneumonia using X-ray images and blood testing data. Frontiers in bioengineering and biotechnology, 11, 1058888.

[12] MayoClinic. (2020) Pneumonia. Accessed: 2023-06-12. [Online]. Available: https://www.mayoclinic.org/diseases-conditions/pneumonia/

[13] VectorStock, (2024). Pneumonia in human lungs vector image. Accessed 2024-03-20. [Online]. Available: https://www.vectorstock.com/royalty-free-vector/pneumonia-in-human-lungs-vector-9914035.

[14] Mujahid, M., Rustam, F., Álvarez, R., Luis Vidal Mazón, J., Díez, I. T., & Ashraf, I. (2022). Pneumonia Classification from X-ray Images with Inception-V3 and Convolutional Neural Network. Diagnostics (Basel, Switzerland), 12(5), 1280.

[15] Aderinto, N., Kokori, E., and Olatunji, G. (2024). A call for reform in Nigerian medical doctors' work hours. Correspondence 403(10428): 726 – 727. https://doi.org/10.1016/S0140-6736(23)02558-8.

[16] Kermany, D.S., Zhang, K., & Goldbaum, M.H. (2018). Large Dataset of Labeled Optical Coherence Tomography (OCT) and Chest X-Ray Images. Accessed: 2022-12-10. [Online]. Available: https://data.mendeley.com/datasets/rscbjbr9sj/2.

[17] Arani, L. A., Sadoughi, F., & Langarizadeh, M. (2019). An Expert System to Diagnose Pneumonia Using Fuzzy Logic. Acta informatica medica: AIM: journal of the Society for Medical Informatics of Bosnia & Herzegovina: casopis Drustva za medicinsku informatiku BiH, 27(2), 103–107.

[18] Singh, A. and Dutta, M. K. (2021) "Diagnosis of Ear Conditions Using Deep Learning Approach. International Conference on Communication, Control and Information Sciences (ICCISc), Idukki, India, 2021, pp. 1-5, doi: 10.1109/ICCISc52257.2021.9484919.

[19] Olatunde O. V. (2024). Pneumonia Severity Diagnosis: A Deep Learning Perspective. Iconic Research and Engineering Journals, 7(7) 414-418.

[20] Alassaf, A. and Yacin Sikkandar, M. (2022). "Intelligent deep transfer learning based malaria parasite detection and classification model using biomedical image," Computers, Materials & Continua. 72(3), pp. 5273–5285.

[21] Elbarougy, R., Aboghrara, E., Behery, G. M., Younes, Y. M., and El-Badry, N.M. (2023). Covid-19 detection on chest x-ray images by combining histogram-oriented gradient and convolutional neural network features. Inf. Sci. Lett, vol. 12, no. 5, pp. 2247–2260.

[22] Barbosa, F., and Canuto, A. (2021). Classification of chest X-ray images using Machine Learning and Histogram of Oriented Gradients. In Anais do XVIII Encontro Nacional de Inteligência Artificial e Computacional, (pp. 49-58). Porto Alegre: SBC.

[23] Parveen, S. and Khan, K. B. (2020). Detection and classification of pneumonia in chest X-ray images by supervised learning. 2020 IEEE 23rd International Multitopic Conference (INMIC), Bahawalpur, Pakistan, 2020, pp. 1-5.

[24] Krishnamoorthy, N., Nirmaladevi, K., Kumaravel, T., Sanjay Nithish, K. S., Sarathkumar, S. and Sarveshwaran, M. (2022). Diagnosis of Pneumonia Using Deep Learning Techniques. 2022 Second International Conference on Advances in Electrical, Computing, Communication and Sustainable Technologies (ICAECT), Bhilai, India, 2022, pp. 1-5.

[25] Siddiqi, R. (2019). Automated pneumonia diagnosis using a customized sequential convolutional neural network," in Proceedings of the 2019 3rd International Conference on Deep Learning Technologies - ICDLT, 2019, pp. 64 –70

[26] Salehi, M., Mohammadi, R., Ghaffari, H., Sadighi, N., and Reiazi, R. (2021). Automated detection of pneumonia cases using deep transfer learning with paediatric chest x-ray images. Br J Radiol, 2021.

[27] Jain, D. K., Singh, T., Saurabh, P., Bisen, D., Sahu, N., Mishra, J., & Rahman, H. (2022). Deep Learning-Aided Automated Pneumonia Detection and Classification Using CXR Scans. Computational intelligence and neuroscience, 2022, 7474304. https://doi.org/10.1155/2022/7474304.